JOURNAL OF MATERIALS SCIENCE 30 (1995) 274–279

Multiple cracking of a coating layer and its influence on fibre strength

Part I *Calculation of the energy release rate of the fibre at cracks for non-uniform crack spacing*

S. OCHIAI, M. HOJO
Mesoscopic Materials Research Centre, Faculty of Engineering, Kyoto University, Kyoto 606, Japan

A calculation method to describe the influence of the non-uniform crack-spacing in a strongly adhering coating layer, which shows multiple cracking, on the energy release rate of a coated fibre is presented and applied to some examples. Four main results were found. The energy release rate of the fibre at the crack in the region of narrow crack-spacing was low. For any crack-spacing, the energy release rate was high when the Young's modulus of the fibre was low and that of the coating layer was high. From the calculation of energy release rates of the fibre at all cracks, the strength-determining crack could be identified, and from this the fibre strength after multiple cracking of the coating layer could be estimated. Finally, the strength of the fibre for non-uniform crack spacing was lower than that for a uniform one.

1. Introduction

When a fibre coated with a strongly adhering brittle coating layer (or a brittle interfacial reaction layer) is pulled in tension, the strength of the fibre is sometimes reduced by the formation of cracks on the fibre surface due to the premature fracture (cracking) of the coating layer [1–8]. Analytical models to describe the reduction in fibre strength have been presented for the case of single cracks [1, 2, 8]. However, in practical fibres, the coating layer shows not only single but also multiple cracks whose influence on fibre strength has not been clarified until now.

In order to describe the strength of coated fibres whose coating layer shows multiple cracks (Fig. 1a), calculation method is required which enables the energy release rate of the fibre, λ, to be estimated at cracks for non-uniform crack-spacings and a method which enables probabilistic affairs to be described, such as crack spacing, location of cracks and the difference in cracking behaviour between samples. The aim of the present work was to present a calculation method for the energy release rate and fibre strength for various non-uniform crack spacings. In Part II [9], the multiple cracking behaviour and its influence on the strength of the fibre will be simulated by means of a Monte Carlo method in combination with the present calculation method.

2. Calculation procedure

2.1. Modelling

The fibre has a radius R_f, length L_f, cross-sectional area S_f, Young's and shear moduli E_f and G_f, respectively, and the coating layer has a thickness a, an inner radius R_f, an outer radius $R_c(=R_f+a)$, cross-sectional area S_c, and Young's and shear moduli, E_c and G_c, respectively. Between the Young's, E, and shear G, moduli, the relation

$$G = E/[2(1+\nu)] \quad (1)$$

is assumed, where ν is the Poisson's ratio.

The shear-lag analysis technique [8, 10–15] was applied for calculation for simplicity. The coated fibre is regarded to be composed of N cylindrical elements, as shown in Fig. 1b. The total number of elements of the fibre and coating layer are N_1 and $N_2(=N-N_1)$, respectively. The element in the centre is numbered 1, the next 2, and then 3, 4, . . . , N, outwards. The cross-sectional area of the ith ($i=1$–N) element is given by S_i. The interface between $i-1$ and i elements is expressed as $(i-1)/i$ interface, as shown in Fig. 1c. The outer and inner radii of the ith element are denoted as R_i and R_{i-1}, respectively, and the distance of the centroid from the inner radius in the ith element as C_i. The Young's and shear moduli of the ith element are denoted E_i and G_i, respectively.

In the longitudinal direction, the total number of cracks in the whole length of the fibre is given by N_f. The segments of the coating layer are numbered $1, 2, \ldots, N_f+1$ and the crack spacing (the length of a segment of coating layer) are denoted L_1, $L_2, \ldots, L_{N_f+1}$ from one end to the other end of the fibre, as shown in Fig. 2a.

The energy release rate, λ, of the fibre at the crack tip will be strongly affected by the crack spacings near the crack considered, but not by those away from the

0022–2461

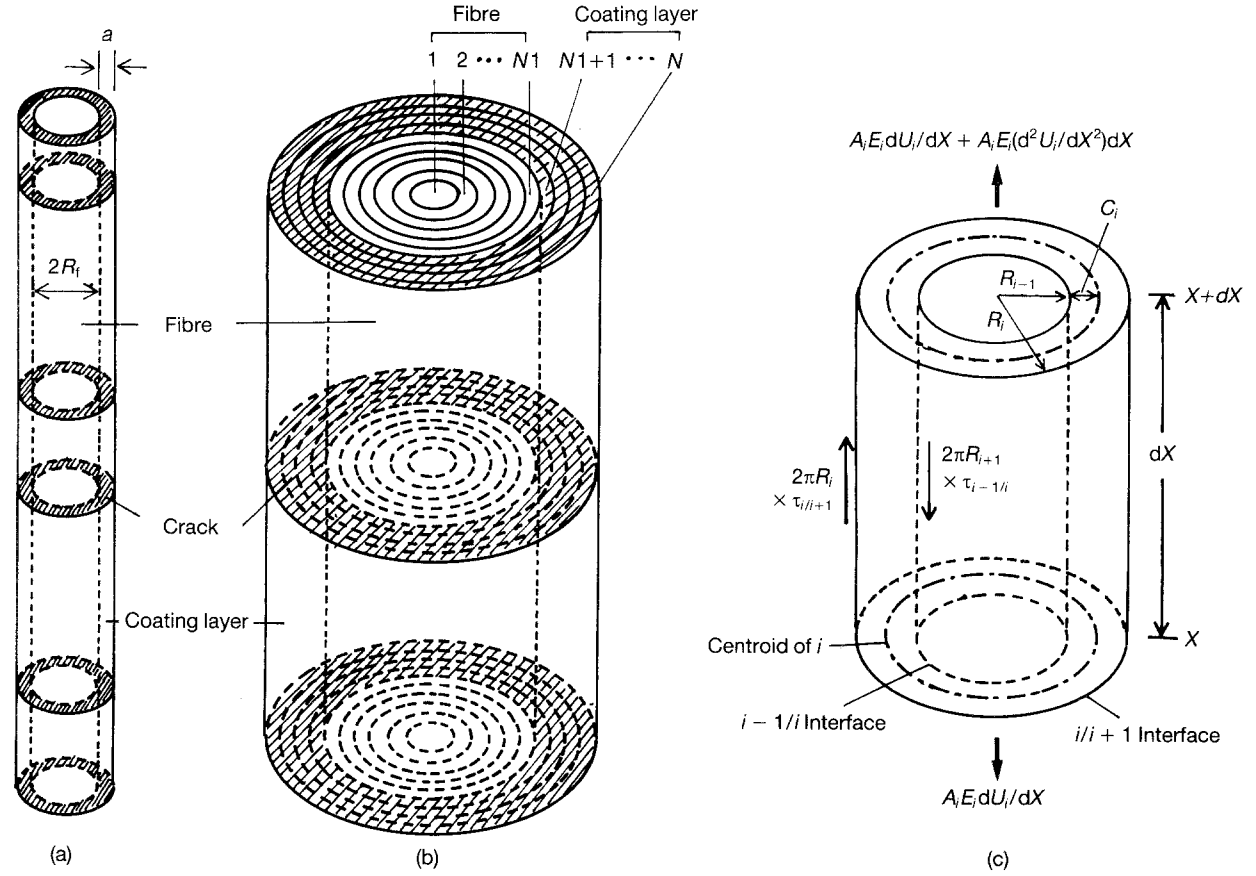

Figure 1 Modelling of the coated fibre for calculation of the strain energy release rate at cracks based on the shear lag analysis. (a) Configuration of the cracked coating layer. (b) Numbering of elements. (c) Stress equlibrium in element i.

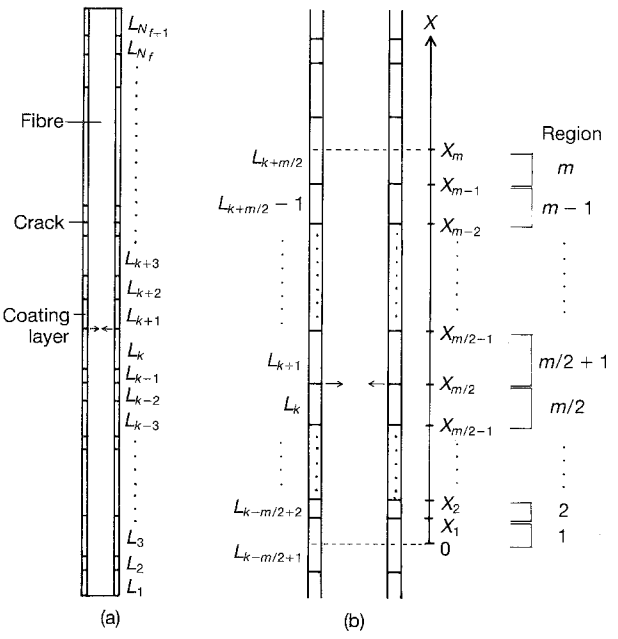

Figure 2 (a) Definition of the length of segments of the coating layer. The segments are numbered from 1 to $N_f + 1$ for the entire length of the fibre, where N_f is the number of cracks. The lengths of the 1 to $N_f + 1$ segments are defined as L_1 *to* L_{N_f+1} respectively. (b) Definition of X for the portion around k and $k + 1$ segments, to calculate the energy release rate at the crack between k and $k + 1$ segments.

crack. To a first approximation, λ at the crack between segments k and $k + 1$ (Fig. 2a) was assumed to be influenced by the number of $m/2$ (m = even) segments below and above the crack, as schematically shown in Fig. 2b. In the calculation, m was taken to be 10 when possible, but it was taken down a place when the operating values during calculation exceeded an allowable magnitude for the computer used.

The distance, X, in the longitudinal direction was defined as follows. The mid-point of the $k - m/2 + 1$ segment was defined to be zero and the mid-point of the $k + m/2$ segment to be X_m. The distances of the cracks were defined as X_1 to X_{m-1}, as shown in Fig. 2b. The X_j ($j = 1$ to $m - 1$) are given by

$$X_1 = (1/2)\,L_{k-m/2+1} \quad (2a)$$

$$X_j = X_{j-1} + L_{k-m/2+j} (j = 2 \text{ to } m - 1) \quad (2b)$$

$$X_m = X_{m-1} + (1/2)\,L_{k+m/2} \quad (2c)$$

The coating layer is cracked at $X = X_1$ to X_{m-1} in the longitudinal direction, as shown in Fig. 2b. The regions covering $0 \leqslant X \leqslant X_1$, $X_1 \leqslant X \leqslant X_2$, ..., $X_{m-1} \leqslant X \leqslant X_m$ were named Regions $1, 2, \ldots, m$, respectively.

2.2. Equilibrium equations

We define the displacement of element i ($i = 1$ to N in Fig. 1b) in Region I ($I = 1$ to m in Fig. 2b) from $X = 0$ as $U_i(I)$. In any regions, the interfacial shear stress at the $i/(i + 1)$ interface, $\tau_{i/(i+1)}{}^{(I)} (i = 1$ to $N - 1)$, is approximately given by [8]

$$\tau_{i/(i+1)}{}^{(I)} = H_i\{U_{i+1}{}^{(I)} - U_i^{(I)}\} \quad (i = 1\text{–}N - 1) \quad (3)$$

$$H_i = G_iG_{i+1}/[G_iC_{i+1} + G_{i+1}(R_i - C_i - R_{i-1})] \quad (4)$$

$\tau_{N/(N+1)}^{(I)}$ is zero, because the outer surface of element N is free (Fig. 1b). From the stress equilibrium shown in Fig. 1c, the following equations are satisfied

$$S_1E_1[d^2U_1^{(I)}/dX^2] + 2\pi R_1\tau_{1/2}^{(I)} = 0 \quad (5)$$

$$S_iE_i[d^2U_i^{(I)}/dX^2] + 2\pi[R_i\tau_{i/(i+1)}^{(I)} - R_{i-1}\tau_{(i-1)/i}^{(I)}] = 0 (i = 2 \text{ to } N-1) \quad (6)$$

$$S_NE_N[d^2U_N^{(I)}/dX^2] - 2\pi R_{N-1}\tau_{(N-1)/N}^{(I)} = 0 \quad (7)$$

In order to obtain a convenient form for the problem, R_i, C_i, S_i, E_i, G_i, H_i, $U_i^{(I)}$, L_q, X and L_f ($i = 1$ to N, $I = 1$–m and $q = k - m/2 + 1$ to $k + m/2$) were converted to the non-dimensional forms r_i, c_i, s_i, e_i, g_i, h_i, $u_i^{(I)}$, l_q, x and l_f, respectively, similar to our previous work [8, 10]. Then the general solution of non-dimensional displacement, $u_i^{(I)}$, was obtained, as shown in the Appendix. The unknown constants, $A_J^{(I)}$'s, ($I = 1$ to m, $J = 1$ to $2N$) in Equation A16 were solved by using the following boundary conditions.

2.3. Boundary conditions

For calculation of the energy release rate at $X = X_{m/2}$ in Fig. 2b whose procedure will be shown later in Section 2.4, the following imaginary cases were considered: case (a) corresponding to the situation before the propagation of the crack at $X = X_{m/2}$ into the fibre, case (b) to the situation after the propagation of the crack by S_{N1} in area (corresponding to the situation when the $N1$ element is broken), and case (c) to the situation after the propagation of the crack by $S_{N1} + S_{N1-1}$ in area (corresponding to the situation when $N1$ and $N1 - 1$ elements are broken). For these cases, the following boundary conditions were used.

1. At $X = 0$, the displacements of all elements are zero.
2. At $X = X_r (r = 1 \text{ to } m - 1)$, the stresses of broken elements ($N_1 + 1$ to N, N_1 to N and $N_1 - 1$ to N for cases (a–c), respectively) are zero, the displacements of unbroken elements (1 to N_1, 1 to $N_1 - 1$ and 1 to $N_1 - 2$ for cases (a–c), respectively) are continuous, and the stress of each element (1 to N) is continuous.
3. The displacements of all elements are equal to each other at $X = X_m$.
4. The load is constant at any cross-section.

2.4. Energy release rate

The energy release rate of the fibre, λ, was calculated by

$$\lambda = (P^2/2)\left\{\lim_{\Delta S \to 0}[C(S + \Delta S) - C(S)]/(\Delta S)\right\} \quad (8)$$

where P is the applied load, S the area of the crack, ΔS the increment of the cross-sectional area of the crack and the $C(S)$ and $C(S + \Delta S)$ are compliances for the crack areas S and $S + \Delta S$, respectively.

At $X = X_m$, the displacement of all elements are taken to be equal to each other as shown in Section 2.3. This assumes that the incremental displacement of the sample due to the crack propagation at $X = X_{m/2}$ is restricted in the region for $0 \leqslant X \leqslant X_m$. Noting the displacements at $X = X_m$ for crack areas S and $S + \Delta S$ as $U(S)$ and $U(S + \Delta S)$, respectively, $[C(S + \Delta S) - C(S)]/\Delta S$ in Equation 8 is approximately given by

$$[C(S + \Delta S) - C(S)]/\Delta S = \{[U(S + \Delta S) - U(S)]/P\}/\Delta S \quad (9)$$

Using the non-dimensional forms of U and S, u and s given by Equations A7 and A3, respectively, Equation 9 is rewritten as

$$[C(S + \Delta S) - C(S)]/\Delta S = [\sigma_f/(\pi R_f)]\{[u(s + \Delta s) - u(s)]/\Delta s\}/P \quad (10)$$

where σ_f is the net fibre stress, given by $P/(\pi R_f)^2$. Substituting Equation 10 and $P = \pi R_f^2\sigma_f$ into Equation 8, we have

$$\lambda = (1/2)(R_f\sigma_f^2)[1/(E_fG_f)]^{1/2} \left\{\lim_{\Delta s \to 0}[u(s + \Delta s) - u(s)]/\Delta s\right\} \quad (11)$$

From Equation 11, λ/σ_f^2 is independent of σ_f. The values of λ/σ_f^2 were calculated as follows. First $u(s)$, where s is the non-dimensional cross-sectional area of the coating layer, was calculated by using the boundary conditions for case (a). Next, Δs (described as Δs_1) was taken to be equal to the non-dimensional cross-sectional area of element N_1, and the $u(s + \Delta s_1)$ was obtained by using the boundary conditions for case (b). Then $\Delta s(\Delta s_2)$ was taken to be the sum of the non-dimensional cross-sectional area of elements N_1 and $N_1 - 1$ and $u(s + \Delta s_2)$ was obtained by using the boundary conditions for case (c). The value of λ was obtained by linear extrapolation to $\Delta s = 0$ in Equation 11.

3. Results and discussion

In the present work, the following values were used as an example: $R_f = 4$ μm, $a = 0.2$ μm, $E_f = 200$ and 400 GPa and $E_c = 100$–600 GPa. The G_f and G_c values were calculated from Equation 1 in which ν for fibre and coating layer was taken to be 0.3. $N2$ was taken to be 12. $N1$ was taken to be the integer of $R_f^2N2/[(R_f + a)^2 - R_f^2]$ when $R_f^2N2/[(R_f + a)^2 - R_f^2] < 41$ and 41 when $R_f^2N2/[(R_f + a)^2 - R_f^2] > 41$ owing to the difficulties of calculation of eigenvalues (Equation A17). In both cases, S_i for $i = 2$ to N were taken to be equal and S_1 was taken to be residual. Such a scheme can be approved because stress in the periphery of the fibre is strongly affected by the crack but not by the inner portion of the fibre away from the interface. This type of approximation in the shear lag analysis is known to be a useful tool for the description of stress distribution in composite materials [14, 15].

3.1. Variation of λ/σ_f^2 with varying length of neighbouring segments of the coating layer

Fig. 3 shows how the λ/σ_f^2 values at a crack are affected by the length of the neighbouring segments of

the coating layer. In this example, the length of one segment, L, is varied under the condition that the lengths of other segments are constant (0.5 μm), as indicated in Fig. 3. The solid arrow shows the crack whose λ/σ_f^2 value was calculated. (In this example, the crack indicated by the dotted arrow is equivalent to that indicated by the solid arrow owing to geometrical symmetry.) The following features are read from Fig. 3.

(i) The smaller is L, the lower λ/σ_f^2 becomes

(ii) The higher the Young's modulus of the fibre, the lower is the λ/σ_f^2.

(iii) The lower Young's modulus of the coating layer, E_c, the lower is λ/σ_f^2.

3.2. λ values at cracks at various locations and the strength of the fibre

The crack-spacing is not uniform when multiple cracking of the coating layer occurs. In this section, as an example, locations of the cracks were assumed as shown in Fig. 4, and the λ/σ_f^2 at the cracks at P_1–P_{10} were calculated for various combinations of E_c and E_f values under a fixed value of $a = 0.2$ μm.

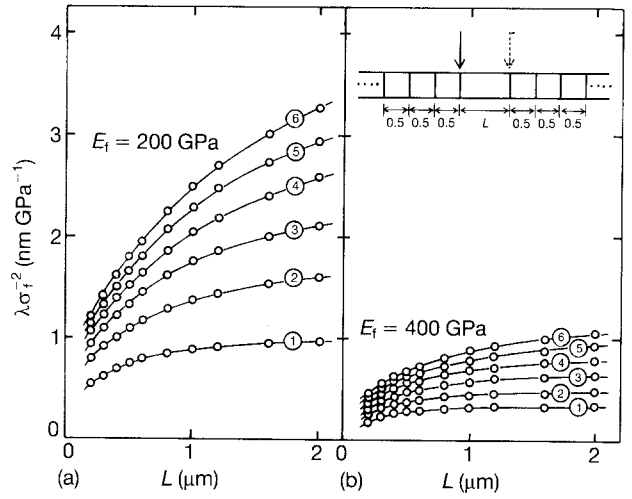

Figure 3 Variations of λ/σ_f^2 at the crack shown by the solid arrow (equivalent to the dotted one) as a function of L for the indicated crack spacing. E_c(GPa): ① 100, ② 200, ③ 300, ④ 400, ⑤ 500, ⑥ 600.

λ is proprotional to σ_f^2, as typically shown in Fig. 5, where 1–4 refer to the cracks at positions P_1–P_4 in Fig. 4. In this example, E_f was taken to be 200 GPa and E_c to be 100 and 400 GPa. Now let us estimate the strength of the fibre and the strength-determining crack by using the example shown in Fig. 5.

Fracture of the fibre occurs when

$$\lambda \geqslant \lambda_c \tag{12}$$

where λ_c is the critical strain energy release rate of the fibre for Mode I fracture. Taking the case of $E_c = 100$ GPa in Fig. 5, if λ_c is 3 J m^{-2}, λ values at P_1–P_4 reach λ_c at A, B, C and D, respectively. Of A–D, C corresponds to the lowest σ_f value at $\lambda = \lambda_c$, which will give the strength of the fibre σ_f^*, if only the cracks at P_1–P_4 are considered. In a similar manner, when $E_c = 400$ GPa, the fibre will be broken at C'. Thus, the fibre strengths are given by the fibre stresses corresponding to C and C', and the crack at P_3 is identified as the strength-determining crack of the four cracks considered. Evidently the strength-determining crack has the highest λ/σ_f^2 value of all the cracks. Fig. 6 shows λ/σ_f^2 values of the cracks at P_1–P_{10} for $E_f = 200$ GPa and $E_c = 400$ GPa as an example. The λ/σ_f^2 value is dependent on the location and is highest at P_7 in this example. Thus, within the positions P_1–P_{10}, the λ value at position P_7 is highest and reaches λ_c at the lowest σ_f value, indicating that the crack at P_7 acts as the strength-determining one. In this way, once the geometry of crack-spacing is known, the fibre strength and strength-determining crack can be known for any number of cracks.

If we assume that the crack spacing is uniform and equal to the average crack spacing, λ/σ_f^2 would be 3.3 nm GPa^{-1}, while it was 4.2 nm GPa^{-1} (P_7 crack) in the case of non-uniform crack spacing (Fig. 6). This means that, in the present non-uniform spacing, the strength predicted from the average crack spacing gives a value about 13% higher than the practical strength value. Thus it should be borne in mind that the strength value based on the average crack spacing tends to give higher predictions.

Fig. 7 shows the influence of the values of E_f and E_c on the λ/σ_f^2 values at P_1–P_4 indicated in Fig. 4. The higher the E_c and the lower the E_f, the higher λ/σ_f^2

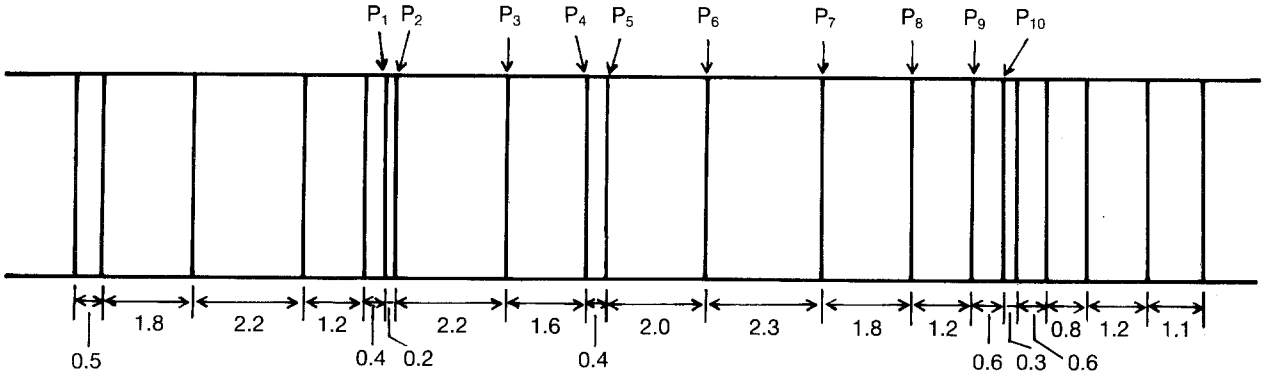

Figure 4 The assumed geometry of crack spacing for the calculation of the energy release rate at the cracks. P_1–P_{10} show the positions of the cracks. The figures 0.5, 1.8, 2.2, etc., show crack spacings.

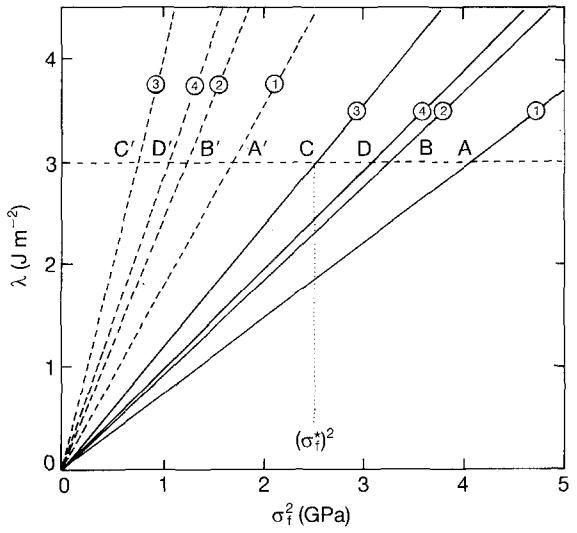

Figure 5 The relationship of λ to σ_f^2 for $E_f = 200$ GPa and $E_c = (——)$ 100 and $(---)$ 400 GPa at positions $P_1$① to $P_4$④ in Fig. 4. If we assume $\lambda_c = 3\ J\ m^{-2}$, the cracks at P_1–P_4 propagate into the fibre at the stresses corresponding to A to D for $E_c = 100$ GPa and A′ to D′ for $E_c = 400$ GPa, respectively.

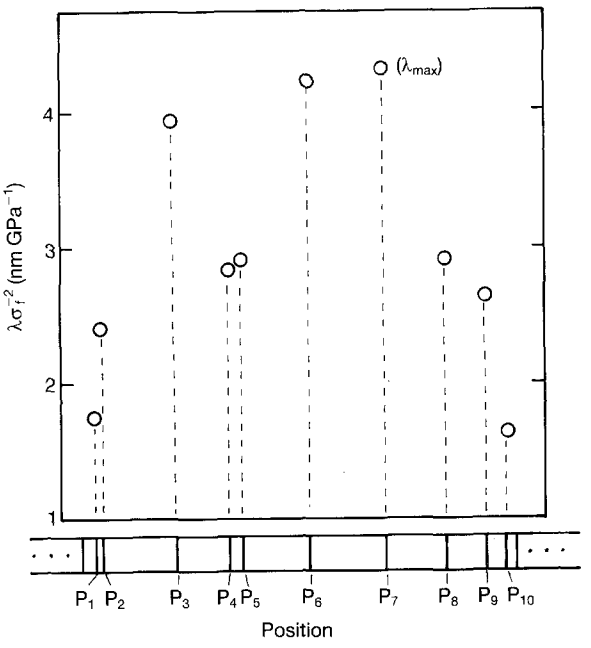

Figure 6 Calculated values of λ/σ_f^2 for the cracks at P_1–P_{10} in Fig. 4, for $E_f = 200$ GPa and $E_c = 400$ GPa. In this example, the crack at P_7 determines strength.

becomes. This suggests that the fibre strength decreases with increasing E_c and decreasing E_f, for a fixed distribution of crack spacing when λ_c is common.

In this work, calculations were performed for some examples under fixed locations of cracks (crack spacings). In practice, the crack spacings in coated fibres vary with increasing applied stress. In Part II [9], the present method will be combined with a Monte Carlo method, and the multiple cracking behaviour of the coating layer as a function of applied stress and its influence on fibre strength will be simulated.

4. Conclusion

A calculation method to describe the influence of multiple cracking of a strongly adhering coating layer on the energy release rates of fibres at the formed cracks has been presented. How much the crack-spacing and the Young's moduli of the fibre and coating layer affect the energy release rate has been demonstrated for specific examples. It was also shown that the strength-determining crack of all the cracks can be identified by the present method, from which the fibre strength after multiple cracking of the coating layer can be estimated.

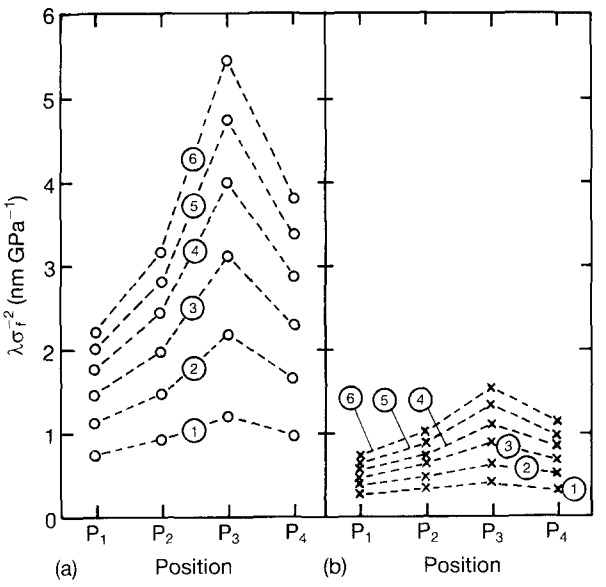

Figure 7 Calculated values of λ/σ_f^2 for the cracks at P_1–P_4 in Fig. 4 for various combinations of the values of E_f and E_c. (a) $E_f = 200$ GPa, (b) $E_f = 400$ GPa. E_c(GPa): ① 100, ② 200, ③ 300, ④ 400, ⑤ 500, ⑥ 600.

Acknowledgement

The authors thank The Ministry of Education, Science and Culture of Japan for a grant-in-aid (04650649).

Appendix

Non-dimensionalization

The following non-dimensionalization was carried for $i = 1$–N, $I = 1$–m and $q = k - m/2 + 1$ to $k + m/2$.

$$R_i = R_f r_i \tag{A1}$$

$$C_i = R_f c_i \{c_i = [(r_i^2 + r_{i-1}^2)/2]^{1/2} - r_{i-1}\} \tag{A2}$$

$$S_i = \pi R_f^2 s_i \tag{A3}$$

$$E_i = E_f e_i \tag{A4}$$

$$G_i = G_f g_i \tag{A5}$$

$$H_i = G_f h_i / R_f$$

$$\{h_i = g_i g_{i+1}/[g_i c_{i+1} + g_{i+1}(r_i - c_i - r_{i-1})]\} \tag{A6}$$

$$U_i^{(I)} = \sigma_f R_f [1/E_f G_f)]^{1/2} u_i^{(I)} \tag{A7}$$

$$L_q = R_f (E_f/G_f)^{1/2} l_q \tag{A8}$$

$$X = R_f (E_f/G_f)^{1/2} x \tag{A9}$$

$$L_f = R_f (E_f/G_f)^{1/2} l_f \tag{A10}$$

where σ_f is the net stress of the fibre, given by $P/(\pi R_f^2)$

where P is the applied load. r_i, c_i, s_i, e_i, g_i, h_i, $u_i^{(I)}$, l_q, x and l_f are non-dimensionalized forms of R_i, C_i, S_i, E_i, G_i, H_i, $U_i^{(I)}$, L_q, X and L_f respectively.

General solution of $u_i^{(I)}$

Substituting Equations A1–A10 into Equations 5–7 and letting

$$2r_ih_i/(e_is_i) = m_i \quad \text{(A11)}$$

$$2r_{i-1}h_{i-1}/(e_is_i) = n_i \quad \text{(A12)}$$

we have the following simplified equations

$$d^2u_1^{(I)}/dx^2 + m_1\{u_2^{(I)} - u_1^{(I)}\} = 0 \quad \text{(A13)}$$

$$d^2u_i^{(I)}/dx^2 + m_iu_{i+1}{}^{(I)} - (m_i + n_i)u_i^{(I)} + n_iu_{i-1}{}^{(I)} = 0 \quad (i = 1 \text{ to } N-1) \quad \text{(A14)}$$

$$d^2u_N^{(I)}/dx^2 - n_N[u_N^{(I)} - u_{N-1}{}^{(I)}] = 0 \quad \text{(A15)}$$

Solving Equations A13–A15, we have the following general solutions of $u_i^{(I)}$.

$$u_i^{(I)} = \sum_{J=1}^{2(N-1)} A_J^{(I)}B_{i,J}\exp(k_Jx) + A_{2N-1}{}^{(I)}x + A_{2N}{}^{(I)} \quad \text{(A16)}$$

where $A_J^{(I)}$s are unknown constants. Of the k_J values ($J = 1$ to $2((N-1))$, the relation of $k_{J+N-1} = -k_J$ (for $J = 1$ to $N-1$) is retained. $(k_J)^2$s ($J = 1$ to $N-1$) are eigenvalues, except zero for the matrix T_N given by

$$T_N = \begin{bmatrix} m_1 & -m_1 & & & & & \\ -n_2 & m_2+n_2 & -m_2 & & & & 0 \\ & -n_3 & m_3+n_3 & -m_3 & & & \\ \cdots\cdots & \cdots\cdots & \cdots\cdots & \cdots\cdots & \cdots\cdots & \cdots\cdots\cdots\cdots\cdots\cdots & \cdots\cdots\cdots\cdots \\ & & & & -n_{N-1} & m_{N-1}+n_{N-1} & -m_{N-1} \\ & 0 & & & & -n_N & n_N \end{bmatrix} \quad \text{(A17)}$$

and $B_{i,J}$s are constants given by

$$B_{1,J} = 1 \quad (J = 1 \text{ to } N-1) \quad \text{(A18)}$$

$$B_{2,J} = (1 - k_J^2/m_1)B_{1,J} \quad (J = 1 \text{ to } N-1) \quad \text{(A19)}$$

$$B_{i,J} = (1 + n_{i-1}/m_{i-1} - k_J^2/m_{i-1})B_{i-1,J} - (n_{i-1}/m_{i-1})B_{i-2,J} \quad (i = 3 \text{ to } N,\ J = 1 \text{ to } N-1) \quad \text{(A20)}$$

The $B_{i,J}$s are common in all regions.

References

1. M. KH. SHORSHOROV, L. M. USTINOV, A. M. ZIRLIN, V. I. OLEFILENCO and L. V. VINOGRADOV, *J. Mater. Sci.* **14** (1979) 1850.
2. J. A. DICARLO, in "Proceedings of the Mechanical Behaviour of Metal/Matrix Composites", edited by J. E. Hack and M. H. Amateau (Metallurgical Society of AIME, Pennsylvania, PA, 1983) pp. 1–14.
3. S. OCHIAI, K. OSAMURA and Y. MURAKAMI, in "Progress in Science and Engineering of Composites", edited by T. Hayashi, K. Kawata and S. Umekawa (Japan Society for Composite Materials, Tokyo, 1982) pp. 1331–8.
4. I. H. KHAN, *Metall. Trans.* **7A** (1976) 1281.
5. W. H. HUNT Jr, in "Interfaces in Metal-Matrix Composites", edited by A. K. Dhingra and S. G. Fishman (Metallurgical Society, Pennsylvania, PA, 1986) pp. 3–25.
6. K. HONJO and A. SHINDO, *J. Mater. Sci.* **21** (1986) 2043.
7. D. D. HIMBEAULT, R. A. VARIN and K. PIEKARSKI, *Metall. Trans.* **20A** (1989) 165.
8. S. OCHIAI, K. OSAMURA and K. HONJO, *Mater. Sci. Eng.* **A158** (1992) 65.
9. S. OCHIAI and K. HOJO, *J. Mater. Sci.* **29** (1994) in press.
10. S. OCHIAI, K. HOJO and K. OSAMURA, *Z. Metallkde*, **84** (1993) 690.
11. J. M. HEDGEPETH, NASA TN D-882 (1961).
12. J. A. NARIN, *J. Compos. Mater.* **22** (1988) 561.
13. H. FUKUDA, in "Achievement in Composite Materials in Japan and the United States" (Prceedings of the 5th Japan–US Conference on Composite Materials), edited by A. Kobayashi, (Japan Society for Composite Materials, Tokyo, 1990) pp. 529–34.
14. C. ZWEBEN, *Eng. Fract. Mech.* **6** (1974) 1.
15. E. D. REEDY Jr, *J. Mech. Phys. Solids* **28** (1980) 265.

Received 18 March 1993
and accepted 9 June 1994